

## Studies of Hydrogen Isotope Accumulation in Plasma Facing Materials Performed in Kurchatov Institute

B.N. Kolbasov 1), M.I. Guseva 1), L.N. Khimchenko 1), B.I. Khripunov 1),  
P.V. Romanov 2), V.G. Stankevich 1), N.Yu. Svechnikov 1), V.I. Vasiliev 3)

1) Kurchatov Institute, Moscow, Russia

2) RF Agency for Atomic Energy, Moscow, Russia

3) Troitsk Institute for Innovative and Thermonuclear Investigations (TRINITI), Troitsk,  
Moscow region, Russia

e-mail contact of main author: [kolbasov@nfi.kiae.ru](mailto:kolbasov@nfi.kiae.ru)

**Abstract.** The report presents an overview of recent Russian studies of hydrogen isotope accumulation in ITER plasma facing materials aiming at search of approaches to decrease tritium retention inside the vacuum vessel of a fusion reactor. These studies address the modeling of plasma interaction with carbon, beryllium, tungsten and their mixtures at both normal fusion reactor operation and at high-intensity deuteron fluxes. Big attention was paid to the hydrogen isotope inventory in the carbon flakes forming inside the tokamak vacuum chamber during the facility operation. Deuterocarbon flakes with atomic ratio  $[D]/[C]$  from 0.002 to values exceeding 1.2 were found inside the T-10 tokamak vacuum chamber. Their color, that is an indicator of the hydrogen concentration varied from black at  $[D]/[C] \leq 0.4$  to reddish-brown at  $[D]/[C] \cong 0.8$  and to yellow at  $[D]/[C]$  above 1.0. Dependence of  $[D]/[C]$  and flake relative mass on temperature of annealing in air and steam was analyzed. Using the Fourier-transform infrared spectroscopy, we found that more than 90% of deuterium atoms in the flakes are in two vibrational states with different binding energies. The first one is characterized by the stretching C-D  $sp^3$  modes at  $2100-2220\text{ cm}^{-1}$  which appear at deuterium concentration above  $[D]/[C] = 0.3$ . The second one is characterized by the weak bending C-D  $sp^3$  modes at  $600$  and  $1100\text{ cm}^{-1}$  at  $[D]/[C] = 0.2-0.3$ . All the C-D  $sp^3$  modes include 2-3 deuterium atoms.  $[D]/[Be]$  in the films redeposited under deuterium plasma interaction with beryllium decreased from 0.15 at 375 K to 0.05 at 575 K. Carbon admixture in Be-D films increases deuterium retention. The formation of mixed Be + C layers on carbon tiles decreases erosion of underlying carbon and hydrogen accumulation. The deuterium concentration in the near-surface layers of tungsten specimens after their exposure to the stationary deuterium plasma, decreased almost by an order of magnitude under exposure to high-energy deuteron fluxes. The deuterium content in tungsten specimens resulting from their exposure to stationary deuterium plasma after preceding exposure to high-energy deuteron fluxes was about two times lower than in specimens that previously were not exposed to such high-energy fluxes.

### 1. Introduction

From our point of view, tritium accumulation in the tokamak vacuum chamber at long working pulses is now the main problem for the International Thermonuclear Experimental Reactor (ITER). A study of the physical-chemical mechanisms determining this accumulation should promote the development of approaches to tritium accumulation reduction. Since we could not carry out experiments with tritium, our experiments were with deuterium. To this end, deuterocarbon (C + D) flakes formed inside the T-10 tokamak, operating at the Kurchatov Institute, were studied. The movable limiter and the fixed diaphragm made of fine-grained pyrolytic graphite MPG-8 were mounted in the tokamak [1, 2].

Experiments for hydrogen isotope accumulation and retention in carbon, beryllium, tungsten and their mixtures were carried out in the facilities LENTA (with a plasma-beam discharge and deuteron energy of 5-10 eV) and VITA (a stationary plasma accelerator) at the Kurchatov Institute, in the magnetron facility MAGRAS at the Institute of Beryllium, and in the electrodynamic accelerator MKT at the Troitsk Institute for Innovative and Thermonuclear Investigations (TRINITI).

## 2. Carbon films formed in the T-10 tokamak

Two types of C + D flakes and films were collected inside the T-10 tokamak vacuum chamber after chamber venting: homogeneous (stratified) flakes and films, and flakes and films composed of globules (globular). Later it was ascertained that there is also the whole spectrum of films with intermediate structures.

The homogeneous films were predominantly located relatively far from the limiter and diaphragm. The difference in colourings of hydrogenated carbon films usually reflects the different hydrogen concentration and different temperatures of film formation. The colour of films formed in the T-10 tokamak varies from black with soot particles on the plasma facing surface (flakes 1) with a  $[D]/[C]$  atomic ratio of  $0.4 \pm 0,2$  at room temperature) to reddish-brown semitransparent (flakes 2 with  $[D]/[C] = 0.8 \pm 0,4$ ) and to yellow with  $[D]/[C] > 1.0$ . The amount of dust in the vacuum chamber was relatively small.

Globular films are formed mainly near the limiter and diaphragm. They conditionally can be considered to have a different age. The ‘young’ globular films have a fractal structure; the microparticles in these films, which have an average size of about 20-30  $\mu\text{m}$ , consist of many smaller microglobules. Those, in turn, are formed from still smaller nanoglobules. The size of the smallest nanoglobules that we observed was 6-8 nm. The  $[D]/[C]$  atomic ratio in such films was up to 0.6. As a result of the high-temperature and irradiation effects, the globular films degrade, losing their internal material in the form of hydrocarbon compounds and forming a microcellular (and quite possible interconnected microporous) structure, consisting mainly of carbon [3]. The  $[D]/[C]$  ratio in these films was reduced to  $(2.0 \pm 0.5) \cdot 10^{-3}$ .

The depth profiles of deuterium concentration were determined by combined secondary-ion mass spectroscopy (SIMS) and residual gas analysis (RGA) technique from both sides of the stratified C + D films collected within T-10 (FIG. 1). The thicknesses of the films were 20-25  $\mu\text{m}$ . The  $[D]/[C]$  atomic ratios in the stratified films increased from the surface value to levels of about 0.4 and 0.8 for films 1 (black) and films 2 (reddish-brown) respectively. In deep layers (more than 250-300 nm from the surface) the  $[D]/[C]$  ratios remain at these levels almost constant. The average values of deuterium concentrations determined by SIMS—RGA and by the elastic recoil detection—Rutherford backscattering methods are in agreement within the experimental uncertainty of 20% for both types of films [4]. The  $[H]/[C]$  atomic ratio in the tokamak flakes varied from 0.1 to 0.6.

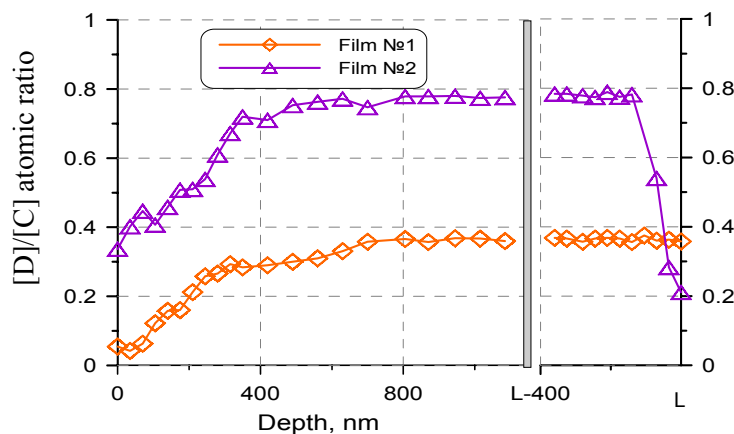


FIG. 1. The  $[D]/[C]$  atomic ratio profiles for stratified C + D flakes collected in the T-10 tokamak vacuum chamber.  $L$  is the total film thickness.

## 2.1 Spectroscopic studies

**Studies at room temperature.** According to the Fourier transform infrared reflectance spectroscopy data [5, 6], the infrared spectra of tokamak films contain the following main vibrational modes:

- the C–H<sub>1,2,3</sub>  $sp^3$  and C–H  $sp^2$  deformation and stretching modes;
- the C–D<sub>2,3</sub>  $sp^3$  deformation and stretching modes;
- the C–C, C=C, C–O and C=O skeletal modes.

More than 90% of D atoms in the stratified flakes are in two vibrational states. At  $[D]/[C] \cong 0.2\text{--}0.3$ , deuterium was found only in the weak C–D<sub>2</sub>  $sp^3$  deformation modes at wave numbers of 633 and 1090  $\text{cm}^{-1}$  while, at higher  $[D]/[C] \approx 0.35\text{--}0.6$ , it was additionally observed in the C–D<sub>2,3</sub>  $sp^3$  stretching modes at 2100–2220  $\text{cm}^{-1}$ , where binding energies are relatively high. Deuterium desorption, which is associated with the breaking of the C–D  $\sigma$  bonds, should start from these high-energy stretching modes at 2073, 2117 and 2217  $\text{cm}^{-1}$ . So, these modes can be used to control the accumulation and desorption of deuterium in co-deposition C + D tokamak films.

Unlike hydrogenated amorphous carbon films, tokamak films hardly produce C–H  $sp^2$  olefinic modes for the C=C linear chains. The C–H  $sp^1$  modes are unresolvable. The C–H<sub>2</sub>D modes were not found among the deuterium-related  $sp^3$  modes. Deuterium was almost absent in the C–D  $sp^2$  aromatic modes. Two or three deuterium atoms attached to a carbon atom are involved in all the C–D<sub>2,3</sub>  $sp^3$  vibrational modes, while one to three protium atoms are involved in the C–H  $sp^2$  and  $sp^3$  vibrational modes. Apparently, since the C–D bonds are more stable than the C–H bonds (isotope-effect), they hamper the loss of more than one deuterium atom, in contrast with the possible loss of one or two protium atoms to form the observable C–D<sub>2,3</sub>  $sp^3$  and C–H<sub>1,2,3</sub>  $sp^3$  modes.

**Annealing at 450°C in nitrogen.** The gravimetric measurements revealed a 29% mass loss on annealing the reddish-brown films at 450°C in nitrogen. The film colour transformed to black, indicating the graphitization of the film. On annealing the films we revealed a noticeable destruction of the C–H<sub>n</sub> aromatic groups in the 700–1000  $\text{cm}^{-1}$  region, a significant decay of the hydroxyl groups (attenuation of O–H modes at 3200–3600 and 1662  $\text{cm}^{-1}$ ), the  $sp^3 \rightarrow sp^2$  process (occurring at  $T > 600$  K) and a reduction in the C–D<sub>2,3</sub> stretching modes in the range 2100–2200  $\text{cm}^{-1}$ .

## 2.2 The behaviour of the deuterium concentration and the relative film mass on annealing the films in air and in water steam

FIG. 2 shows the effect of annealing in the atmospheric air on the  $[D]/[C]$  atomic ratio in hydrogenated stratified carbon films. The annealing took place at fixed temperatures with 50 K intervals for 32 h. The duration of the annealing was determined by the requirement of the ITER Joint Central Team. The temperature in the autoclave was controlled with an accuracy of 0.5 K. New films were used for each temperature step of the annealing. The concentrations measured by Causey *et al.* [7] after the films had been annealed in air for 0.5 h are shown in FIG. 2 for comparison with our data. The reduction of D concentration in both types of films at their annealing in steam is very close to that at annealing in air.

The film masses were determined before and after annealing in air and water steam using an electronic microbalance with an accuracy of  $\pm 1$   $\mu\text{g}$ . The film mass after annealing at the

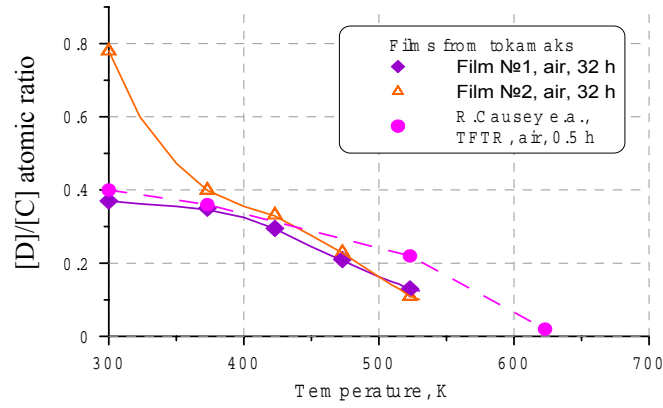


FIG. 2. Comparison of the  $[D]/[C]$  atomic ratio variations in stratified hydrogenated carbon films produced in tokamaks versus the annealing temperature in air. The films collected in T-10 were annealed for 32 h; the films from TFTR were annealed for 0.5 h.

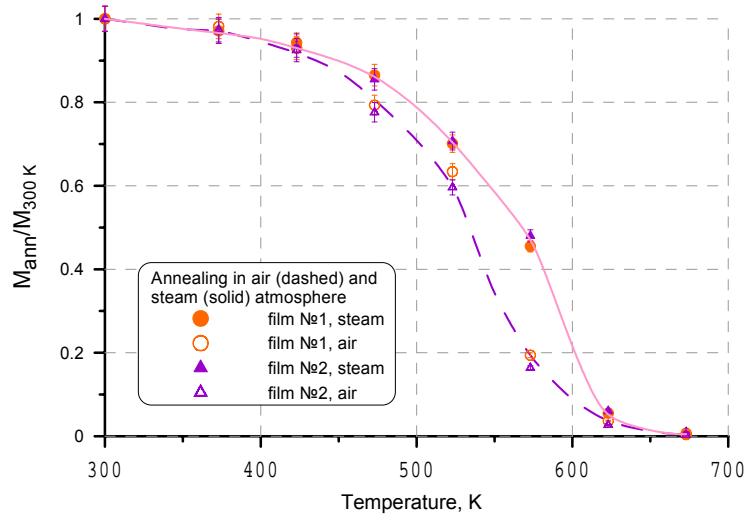


FIG. 3. The relative masses of stratified hydrogenated carbon films annealed for 32 h in steam (solid curves) and in air (dashed curves) versus the annealing temperature

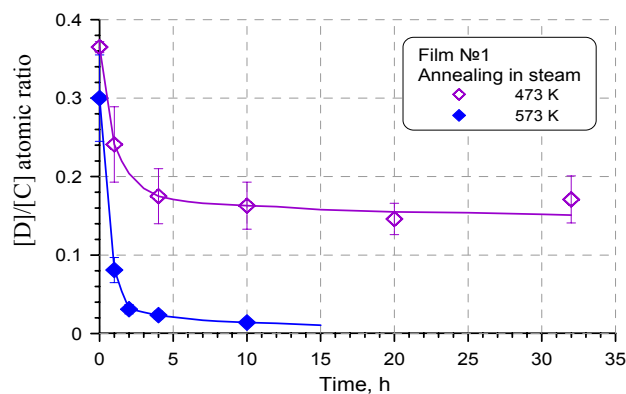


FIG. 4. The reduction in the  $[D]/[C]$  atomic ratio in D + C films 1 on annealing in steam at  $T = 473$  and  $573$  K as a function of the annealing duration.

temperature  $T$  was referred to the mass  $M_{300\text{ K}}$  determined at the room temperature. The dependences of the mass losses on annealing temperature for both types of tested films are almost the same. Generally, at the same temperatures the mass losses after annealing in steam are lower than after annealing in air (see FIG. 3).

For both types of films the patterns of time dependencies of a  $[D]/[C]$  atomic ratio reduction under annealing in air and steam are very similar. The main deuterium release takes place during the first 4 h when under annealing at 473 K a  $[D]/[C]$  ratio decreases from the original values of  $\sim 0.4$  (in film 1) and  $\sim 0.8$  (in film 2) to  $\sim 0.15$ – $0.2$ . Further the  $[D]/[C]$  ratios are almost constant (see FIG. 4). At higher annealing temperatures, deuterium releases more quickly. During the first 4 h of annealing at 573 K, the  $[D]/[C]$  ratio decreases to  $0.025 - 0.03$ .

### 3. Hydrogen isotope accumulation in beryllium

Analysis of re-deposited Be layers in experiments simulating normal ITER operation in the magnetron sputtering facility MAGRAS in the Beryllium Institute has shown that the  $[D]/[Be]$  atomic ratio in the layers under consideration decreases from 0.15 at the temperature  $T = 375$  K to 0.05 at 575 K (FIG. 5) [8]. In this temperature range the atomic ratio

$$[D]/[Be] = 0.34 - 0.0005 T.$$

An example of the depth distribution of chemical elements in a re-deposited beryllium layer is shown in FIG. 6 [10].

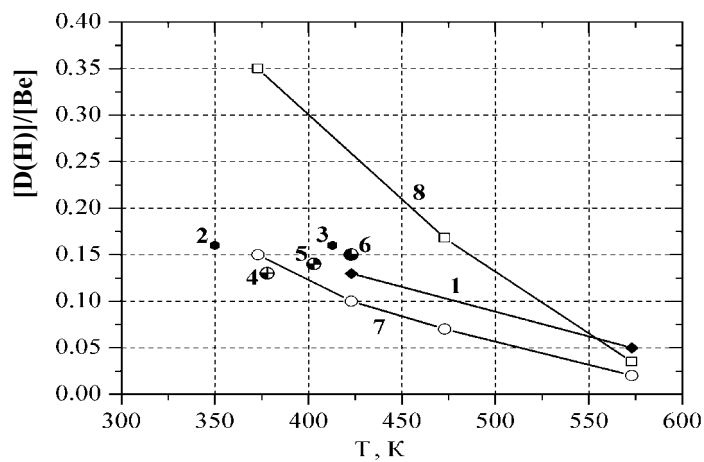


FIG. 5. The  $[D(H)]/[Be]$  atomic ratio in re-deposited layers: line 1, homogeneous beryllium target; points 2 and 3, beryllium targets contaminated with hydrocarbons; points 4, 5 and 6, compound Be-W targets with different Be:W surface area ratios (point 4, 3:1; point 5, 1:1; point 6, 1:3); lines 7 and 8, data obtained by Causey and Walsh [9] (line 7, with lower oxygen concentration; line 8, with higher oxygen concentration).

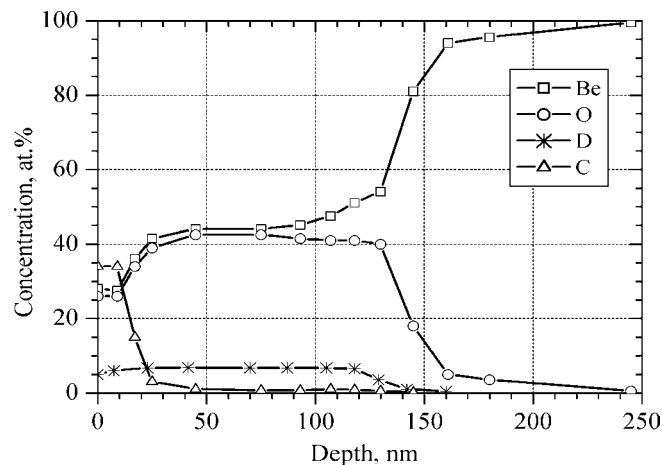


FIG. 6. The depth distribution of chemical elements in the re-deposited beryllium layer.

## 5. Hydrogen isotope accumulation in tungsten in a simulation of the normal ITER operation and plasma disruptions

Deuterium accumulation in the near-surface layer of polycrystalline tungsten in its interaction with stationary deuterium plasma in the LENTA facility (Kurchatov Institute) was studied [11]. The deuteron energy was about 200 eV, the current density on the target  $5 \times 10^{21} \text{ m}^{-2} \cdot \text{s}^{-1}$  and the deuteron exposure dose  $10^{26} \text{ m}^{-2}$ . The temperature of the specimens under exposure was 800 K. To measure the integral deuterium concentration and the profiles of its distribution in tungsten, W specimens were irradiated in a Van de Graaff accelerator by  $\text{He}^+$  ions. Recoil atoms were recorded with a semiconductor detector. The integral deuterium concentration in tungsten after its exposure to stationary deuterium plasma was  $1.5 \times 10^{20} \text{ m}^{-2}$ . The depth distribution of D in the near-surface tungsten layer 60-nm thick is shown in FIG. 7.

To study the plasma disruption effect on deuterium accumulation in the near-surface tungsten layer, after exposure of tungsten specimens to stationary deuterium plasma in the LENTA facility, they were bombarded by powerful pulsed fluxes of deuterium plasma, imitating plasma disruptions, in the electrodynamic plasma accelerator MKT. The deuterium plasma density was about  $10^{21} \text{ m}^{-3}$ , and the maximum deuteron energy was 1–2 keV. The pulse duration was about 60  $\mu\text{s}$ . The integral D concentration decreased by almost an order of magnitude (to  $2 \times 10^{19} \text{ m}^{-2}$ ) under ten pulses (with an energy flux density of 0.5 MJ/m<sup>2</sup> each) (see FIG. 7). The pattern of the D atom distribution in W (the profile shift to the surface on simulation of plasma disruption) shows that D diffusion in these conditions takes place only towards the surface, resulting in the release of a large part of the D from tungsten into the vacuum chamber. The deuterium was retained only in a narrow surface layer approximately 10 nm thick. Then the same specimens were once again exposed to stationary D plasma in the LENTA facility with the above-mentioned exposure parameters. The integral concentration of D in the specimens became equal to  $7 \times 10^{19} \text{ m}^{-2}$  or was about half that in specimens which had not previously been exposed to the fluxes simulating plasma disruptions [11].

The exposure of W doped with different elements in stationary D plasma at 770 K to a dose of  $10^{25} \text{ m}^{-2}$  (FIG. 8) has shown that doping affects the D concentration in tungsten surface layers. The deuterium concentration in tungsten doped with  $\text{La}_2\text{O}_3$  is less than in tungsten doped with rhenium and in single-crystal W(111). In W doped with titanium and yttrium, deuterium has the lowest concentration but uniform distribution (see FIG. 8, curve 1) [12].

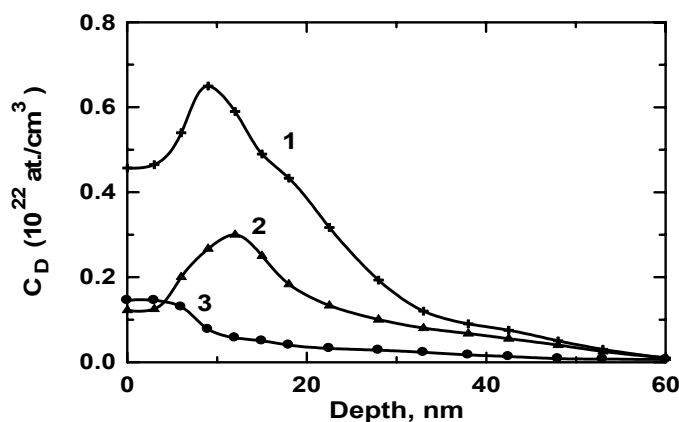


FIG. 7. The depth distribution of D in W near-surface layer: curve 1, after irradiation by stationary D plasma; curve 2, after irradiation by stationary D plasma + pulsed D plasma + stationary D plasma; curve 3, after irradiation by stationary D plasma + pulsed deuterium plasma [11].

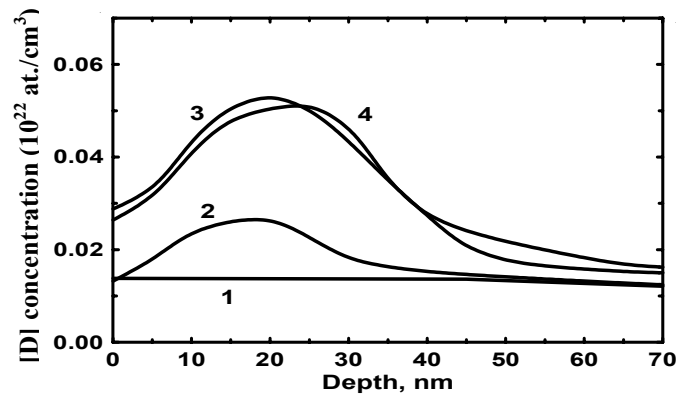


FIG. 8. The depth distributions of deuterium in the surface layers after exposure in a stationary deuterium plasma at 770 K to the dose  $D = 10^{25} \text{ m}^{-2}$ : curve 1, W-13I, doped with titanium and yttrium; curve 2, W-1%  $\text{La}_2\text{O}_3$ ; curve 3, W-10% Re; curve 4, single-crystal W(111).

Deuterium was not detected in tungsten specimens exposed to powerful pulsed fluxes of deuterium plasma simulating plasma disruptions without preceding or subsequent exposure to stationary deuterium plasma imitating normal ITER operation. However, the same high power plasma treatment of carbon-coated tungsten results in full destruction of the carbon layer (250 nm) and in the formation of a mixed C+W layer near the tungsten surface. Deuterium is retained in this mixed layer only. Its integral concentration is  $3 \times 10^{19} \text{ m}^{-2}$  [12].

Deuterium accumulation in a mixed W + Be layer on a beryllium substrate (35 at.% Be + 35 at.% W + 30 at.% O) was studied with simulation of plasma disruptions in the plasma accelerator MKT (density of energy flux, 200  $\text{kJ/m}^2$ ). Deuterium was located only in the surface layer 150-nm thick. It is absent in the beryllium substrate because of its release outwards during melting of the mixed layer. Formation of the W + Be layer on the beryllium first wall at normal ITER operation and its removal at plasma disruptions will decrease the accumulation of hydrogen isotopes in Be and prevent their diffusion into the Be bulk [13].

## 6. Discussion of results and conclusion

The results of studies described in the paper can be interpreted as follows.

- The main mechanism of the accumulation and retention of hydrogen isotopes inside the tokamak vacuum chamber is hydrogen co-deposition with eroded carbon. Homogeneous deuterocarbon flakes and films resulted from such a co-deposition have rather high  $[\text{D}]/[\text{C}]$  atomic ratio (from 0.4 to above 1.0 at room temperature). Under continuing plasma irradiation these flakes and films are transformed into globular flakes and films, and the deuterium content in them decreases. One of the most radical means to reduce the content of hydrogen isotopes is to increase the temperature. The flakes, which are not affected by irradiation and temperature retain accumulated hydrogen.
- At accidents temperature build up accompanied by ingress of steam or air into the vacuum chamber of a tokamak, the  $[\text{D}]/[\text{C}]$  atomic ratio and the mass of carbon flakes decrease depending on the temperature. The reduction in the  $[\text{D}]/[\text{C}]$  atomic ratio is almost independent on the atmosphere (air or steam). Mass losses of C + D flakes in the steam are less than in air at the same temperatures.
- More than 90% of deuterium atoms in the homogeneous flakes are in two vibrational states. At  $[\text{D}]/[\text{C}] \approx 0.2\text{--}0.3$ , deuterium was found only in the weak  $\text{C}\text{--D}_2 \text{ sp}^3$  deformation modes at wave numbers of 633 and 1090  $\text{cm}^{-1}$  while, at  $[\text{D}]/[\text{C}] \approx (0.35\text{--}0.6)$ , it was additionally observed in the  $\text{C}\text{--D}_{2,3} \text{ sp}^3$  stretching modes at 2100-2220  $\text{cm}^{-1}$ . Deuterium

desorption, which is associated with the breaking of the C–D  $\sigma$  bonds, should start from these high-energy stretching modes at 2073, 2117 and 2217  $\text{cm}^{-1}$ .

- Co-deposition of hydrogen isotopes with eroded beryllium is somewhat less than with carbon, but its level is approximately the same ( $[\text{D}]/[\text{Be}]$  atomic ratio of 0.15 at  $T = 375 \text{ K}$ ). The carbon impurities in the Be + D films slightly increase the D retention.
- Accumulation of hydrogen isotopes in tungsten is not essential. During a plasma disruption the hydrogen isotope concentration in tungsten decreases. After plasma disruption, accumulation of hydrogen isotopes in W is less than before the disruption.
- Among different tungsten materials the lowest deuterium concentration was found in tungsten doped with titanium and yttrium; the highest deuterium concentration was in tungsten doped with rhenium.

## References

- [1] ROMANOV, P.V., et al., “Microstructure and deuterium content of tokamak T-10 carbon erosion products”, *J. Nucl. Mater.* **307-311** (2002) 1294.
- [2] ALIMOV, V.KH. et al., “Studies of structure and deuterium content of carbon films re-deposited in tokamak T-10 vacuum chamber”, *Problems of Atomic Science and Engineering, Ser. Thermonuclear Fusion, Moscow* (2000) No. 2, 45-55 (in Russian).
- [3] GUSEVA, M.I., et al., “Microstructure features and deuterium content in carbon globular films re-deposited in T-10 tokamak”, *Problems of Atomic Science and Engineering, Ser. Thermonuclear Fusion, Moscow* (2001) № 1, 3-12 and <http://www.design.tokamak.ru/vant/htm> (in Russian).
- [4] KOLBASOV, B.N., et al., “Deuterium mobilization from co-deposited carbon films produced in T-10 tokamak”, *ITER Russian Federation Home Team Report RF 1 F 226 14/06/01 E*, Kurchatov Institute, Moscow (2001).
- [5] SVECHNIKOV, N.YU., et al., “Spectroscopic studies of homogeneous thin carbon erosion films and flakes with a high deuterium content formed in tokamak T-10”, *Fus. Eng. Des.* **75-79** (2005) 339.
- [6] SVECHNIKOV, N.YU., et al., “Temperature and spectroscopic characteristics of homogeneous co-deposited carbon-deuterium films produced in the T-10 tokamak”, *Plasma Devices and Operations* **14** (2006) 137.
- [7] FEDERICI, G., et al., “Tritium inventory in the ITER PFC’s: predictions, uncertainties, R&D status and priority needs”, *Fus. Eng. Des.* **39&40** (1998) 445.
- [8] ZIMIN, A.M., et al., “Modeling of beryllium sputtering and re-deposition in fusion reactor plasma facing components”, *J. Nucl. Mater.* **329-333** (2004) 855.
- [9] CAUSEY, R.A., WALSH, D.S., “Co-deposition of deuterium with beryllium”, *J. Nucl. Mater.* **254** (1998) 84.
- [10] ZIMIN, A.M., et al., “Modeling of hydrogen isotope ion interaction with beryllium plasma facing armour”, *Plasma Devices and Operation*, **12** (2004) 89.
- [11] KORSHUNOV, S.N., et al., “Deuterium behaviour in tungsten and graphite at combined stationary and powerful pulsed plasma flow action”, *Hydrogen Recycling at Plasma Facing Materials (Proc. Int. Workshop Tokyo, 1998)*, University of Tokyo, UTNL-R0380, 161-176 (1998).
- [12] KOLBASOV, B.N., et al., “Fusion safety studies in Russia from 1996 to 2000”, *Fusion Eng. Des.* **54** (#3-4) (2001) 451.
- [13] KORSHUNOV, S.N., et al., “Deuterium accumulation in mixed W—Be layers on Be and morphological features of their erosion products in experiments on plasma disruption simulation”, *Problems of Atomic Science and Engineering, Ser. Thermonuclear Fusion, Moscow* (1999) № 2, 47-52 and <http://www.design.tokamak.ru/vant/htm> (in Russian).